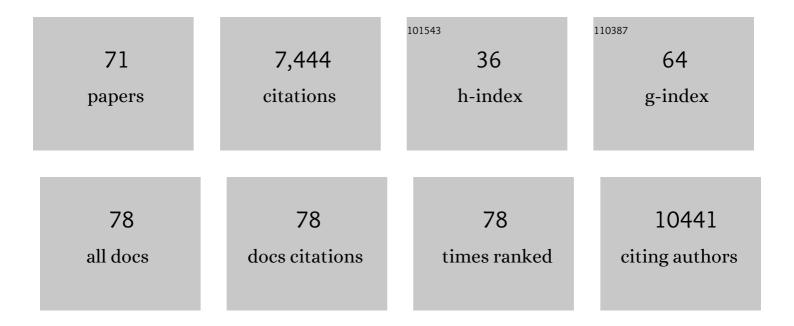
List of Publications by Year in descending order

Source: https://exaly.com/author-pdf/8044498/publications.pdf

Version: 2024-02-01



| #  | Article  | IF   | CITATIONS |
|----|--|------|-----------|
| 1  | Unified Polymerization Mechanism for the Assembly of ASC-Dependent Inflammasomes. Cell, 2014, 156, 1193-1206.  | 28.9 | 1,035     |
| 2  | Recognition Dynamics Up to Microseconds Revealed from an RDC-Derived Ubiquitin Ensemble in Solution. Science, 2008, 320, 1471-1475.  | 12.6 | 963       |
| 3  | Fibril structure of amyloid-β(1–42) by cryo–electron microscopy. Science, 2017, 358, 116-119.  | 12.6 | 801       |
| 4  | Single-molecule fluorescence resonance energy transfer reveals a dynamic equilibrium between<br>closed and open conformations of syntaxin 1. Proceedings of the National Academy of Sciences of the<br>United States of America, 2003, 100, 15516-15521. | 7.1  | 268       |
| 5  | Super-resolution biomolecular crystallography with low-resolution data. Nature, 2010, 464, 1218-1222.  | 27.8 | 267       |
| 6  | Combining Efficient Conformational Sampling with a Deformable Elastic Network Model Facilitates<br>Structure Refinement at Low Resolution. Structure, 2007, 15, 1630-1641.   | 3.3  | 213       |
| 7  | Mechanism of folding chamber closure in a group II chaperonin. Nature, 2010, 463, 379-383.   | 27.8 | 196       |
| 8  | Remodeling of actin filaments by ADF/cofilin proteins. Proceedings of the National Academy of Sciences of the United States of America, 2011, 108, 20568-20572.  | 7.1  | 194       |
| 9  | Structure of Myxovirus Resistance Protein A Reveals Intra- and Intermolecular Domain Interactions<br>Required for the Antiviral Function. Immunity, 2011, 35, 514-525.   | 14.3 | 188       |
| 10 | Single-molecule FRET measures bends and kinks in DNA. Proceedings of the National Academy of Sciences of the United States of America, 2008, 105, 18337-18342.   | 7.1  | 172       |
| 11 | Structural polymorphism in F-actin. Nature Structural and Molecular Biology, 2010, 17, 1318-1323.  | 8.2  | 170       |
| 12 | Outcome of the First wwPDB Hybrid/Integrative Methods Task Force Workshop. Structure, 2015, 23, 1156-1167.   | 3.3  | 159       |
| 13 | Energy barriers and driving forces in tRNA translocation through the ribosome. Nature Structural and Molecular Biology, 2013, 20, 1390-1396.   | 8.2  | 150       |
| 14 | Simulation of Fluorescence Anisotropy Experiments: Probing Protein Dynamics. Biophysical Journal, 2005, 89, 3757-3770.   | 0.5  | 128       |
| 15 | Near-Atomic Resolution for One State of F-Actin. Structure, 2015, 23, 173-182.   | 3.3  | 121       |
| 16 | Cryo-EM structure of islet amyloid polypeptide fibrils reveals similarities with amyloid-β fibrils. Nature<br>Structural and Molecular Biology, 2020, 27, 660-667.   | 8.2  | 120       |
| 17 | Visualizing GroEL/ES in the Act of Encapsulating a Folding Protein. Cell, 2013, 153, 1354-1365.  | 28.9 | 102       |
| 18 | Amyloid-type Protein Aggregation and Prion-like Properties of Amyloids. Chemical Reviews, 2021, 121, 8285-8307.  | 47.7 | 98        |

| #  | Article  | IF   | CITATIONS |
|----|--|------|-----------|
| 19 | The pathway to GTPase activation of elongation factor SelB on the ribosome. Nature, 2016, 540, 80-85.  | 27.8 | 93        |
| 20 | Symmetry-free cryo-EM structures of the chaperonin TRiC along its ATPase-driven conformational cycle. EMBO Journal, 2012, 31, 720-730.   | 7.8  | 80        |
| 21 | Cryo-EM model validation recommendations based on outcomes of the 2019 EMDataResource challenge. Nature Methods, 2021, 18, 156-164.  | 19.0 | 73        |
| 22 | Ca <sup>2+</sup> -induced movement of tropomyosin on native cardiac thin filaments revealed by cryoelectron microscopy. Proceedings of the National Academy of Sciences of the United States of America, 2017, 114, 6782-6787. | 7.1  | 63        |
| 23 | Maximum likelihood trajectories from single molecule fluorescence resonance energy transfer experiments. Journal of Chemical Physics, 2003, 119, 9920-9924.  | 3.0  | 62        |
| 24 | The Crystal Structures of the Eukaryotic Chaperonin CCT Reveal Its Functional Partitioning.<br>Structure, 2013, 21, 540-549.   | 3.3  | 59        |
| 25 | Ligand-induced structural changes in the cyclic nucleotide-modulated potassium channel MloK1.<br>Nature Communications, 2014, 5, 3106.   | 12.8 | 59        |
| 26 | Endo-lysosomal AÎ <sup>2</sup> concentration and pH trigger formation of AÎ <sup>2</sup> oligomers that potently induce Tau missorting. Nature Communications, 2021, 12, 4634.   | 12.8 | 59        |
| 27 | N-Terminal Domains of Cardiac Myosin Binding Protein C Cooperatively Activate the Thin Filament.<br>Structure, 2018, 26, 1604-1611.e4.   | 3.3  | 57        |
| 28 | Engineering and application of a biosensor with focused ligand specificity. Nature Communications, 2020, 11, 4851.   | 12.8 | 56        |
| 29 | A Spring-loaded Release Mechanism Regulates Domain Movement and Catalysis in Phosphoglycerate<br>Kinase. Journal of Biological Chemistry, 2011, 286, 14040-14048.  | 3.4  | 53        |
| 30 | Realâ€space refinement with DireX: From global fitting to sideâ€chain improvements. Biopolymers, 2012, 97,<br>687-697.   | 2.4  | 52        |
| 31 | Archaeal flagellin combines a bacterial type IV pilin domain with an Ig-like domain. Proceedings of the<br>National Academy of Sciences of the United States of America, 2016, 113, 10352-10357.                               | 7.1  | 49        |
| 32 | Detecting protein-induced folding of the U4 snRNA kink-turn by single-molecule multiparameter FRET measurements. Rna, 2005, 11, 1545-1554.   | 3.5  | 46        |
| 33 | Branchpoint Expansion in a Fully Complementary Three-Way DNA Junction. Journal of the American<br>Chemical Society, 2012, 134, 6280-6285.  | 13.7 | 44        |
| 34 | Cross-validation in cryo-EM–based structural modeling. Proceedings of the National Academy of<br>Sciences of the United States of America, 2013, 110, 8930-8935.   | 7.1  | 42        |
| 35 | High-Resolution Cryo-EM Structure of the Cardiac Actomyosin Complex. Structure, 2021, 29, 50-60.e4.  | 3.3  | 41        |
| 36 | Filaments from Ignicoccus hospitalis Show Diversity of Packing in Proteins Containing N-Terminal<br>Type IV Pilin Helices. Journal of Molecular Biology, 2012, 422, 274-281.   | 4.2  | 40        |

| #  | Article   | IF   | CITATIONS |
|----|---|------|-----------|
| 37 | Atomistic structure and dynamics of the human MHC-I peptide-loading complex. Proceedings of the National Academy of Sciences of the United States of America, 2020, 117, 20597-20606.   | 7.1  | 40        |
| 38 | Improving the Accuracy of Macromolecular Structure Refinement at 7ÂÃ Resolution. Structure, 2012, 20, 957-966.  | 3.3  | 37        |
| 39 | Hybrid methods for macromolecular structure determination: experiment with expectations. Current<br>Opinion in Structural Biology, 2015, 31, 20-27.   | 5.7  | 37        |
| 40 | Architecture of the flexible tail tube of bacteriophage SPP1. Nature Communications, 2020, 11, 5759.  | 12.8 | 37        |
| 41 | Major tail proteins of bacteriophages of the order Caudovirales. Journal of Biological Chemistry, 2022, 298, 101472.  | 3.4  | 37        |
| 42 | Global Structure of Forked DNA in Solution Revealed by High-Resolution Single-Molecule FRET.<br>Journal of the American Chemical Society, 2011, 133, 1188-1191.   | 13.7 | 36        |
| 43 | β-Hairpin of Islet Amyloid Polypeptide Bound to an Aggregation Inhibitor. Scientific Reports, 2016, 6,<br>33474.  | 3.3  | 34        |
| 44 | Atomic structure of PI3-kinase SH3 amyloid fibrils by cryo-electron microscopy. Nature Communications, 2019, 10, 3754.  | 12.8 | 32        |
| 45 | Deformable elastic network refinement for low-resolution macromolecular crystallography. Acta<br>Crystallographica Section D: Biological Crystallography, 2014, 70, 2241-2255.  | 2.5  | 29        |
| 46 | Integrated NMR, Fluorescence, and Molecular Dynamics Benchmark Study of Protein Mechanics and<br>Hydrodynamics. Journal of Physical Chemistry B, 2019, 123, 1453-1480.  | 2.6  | 29        |
| 47 | Application of DEN refinement and automated model building to a difficult case of molecular-replacement phasing: the structure of a putative succinyl-diaminopimelate desuccinylase from <i>Corynebacterium glutamicum</i> . Acta Crystallographica Section D: Biological Crystallography, 2012, 68, 391-403. | 2.5  | 26        |
| 48 | The refined structure of functional unit h of keyhole limpet hemocyanin (KLH1â€h) reveals disulfide bridges. IUBMB Life, 2011, 63, 183-187.   | 3.4  | 23        |
| 49 | Integrating cryo-EM and NMR data. Current Opinion in Structural Biology, 2020, 61, 173-181.   | 5.7  | 23        |
| 50 | The <i>Uppsala APP</i> deletion causes early onset autosomal dominant Alzheimer's disease by altering APP processing and increasing amyloid β fibril formation. Science Translational Medicine, 2021, 13, .   | 12.4 | 23        |
| 51 | Archaeal actin from a hyperthermophile forms a single-stranded filament. Proceedings of the National Academy of Sciences of the United States of America, 2015, 112, 9340-9345.   | 7.1  | 22        |
| 52 | FRETsg: Biomolecular structure model building from multiple FRET experiments. Computer Physics<br>Communications, 2004, 158, 150-157.   | 7.5  | 20        |
| 53 | Challenges in sample preparation and structure determination of amyloids by cryo-EM. Journal of Biological Chemistry, 2021, 297, 100938.  | 3.4  | 20        |
| 54 | A grid-enabled web service for low-resolution crystal structure refinement. Acta Crystallographica<br>Section D: Biological Crystallography, 2012, 68, 261-267.   | 2.5  | 17        |

| #  | Article  | IF  | CITATIONS |
|----|--|-----|-----------|
| 55 | Improving the visualization of cryo-EM density reconstructions. Journal of Structural Biology, 2015, 191, 207-213.   | 2.8 | 17        |
| 56 | Conformational Heterogeneity in a Fully Complementary DNA Three-Way Junction with a GC-Rich<br>Branchpoint. Biochemistry, 2017, 56, 4985-4991.   | 2.5 | 12        |
| 57 | Small-angle X-ray Scattering of Apolipoprotein A-IV Reveals the Importance of Its Termini for Structural Stability. Journal of Biological Chemistry, 2013, 288, 4854-4866.                     | 3.4 | 10        |
| 58 | Protein structure refinement with adaptively restrained homologous replicas. Proteins: Structure,<br>Function and Bioinformatics, 2016, 84, 302-313.   | 2.6 | 10        |
| 59 | Clustering polymorphs of tau and IAPP fibrils with the CHEP algorithm. Progress in Biophysics and Molecular Biology, 2021, 160, 16-25.   | 2.9 | 10        |
| 60 | α-Synuclein-derived lipoparticles in the study of α-Synuclein amyloid fibril formation. Chemistry and<br>Physics of Lipids, 2019, 220, 57-65.  | 3.2 | 9         |
| 61 | Clustering cryo-EM images of helical protein polymers for helical reconstructions. Ultramicroscopy, 2019, 203, 132-138.  | 1.9 | 9         |
| 62 | Conformational heterogeneity coupled with $\hat{l}^2$ -fibril formation of a scaffold protein involved in chronic mental illnesses. Translational Psychiatry, 2021, 11, 639.                   | 4.8 | 9         |
| 63 | Coupling an Ensemble of Homologues Improves Refinement of Protein Homology Models. Journal of Chemical Theory and Computation, 2015, 11, 5578-5582.  | 5.3 | 4         |
| 64 | Remodeling of Actin Filaments by Cofilin. Biophysical Journal, 2012, 102, 238a.  | 0.5 | 0         |
| 65 | Dynamic, Energetic, and Kinetic Determinants of Ribosomal Translocation: Microsecond All-Atom<br>Simulations of Hybrid Cryoem/X-Ray Structural Substates. Biophysical Journal, 2012, 102, 67a. | 0.5 | 0         |
| 66 | Mechanisms for Efficient TRNA Translocation through the Ribosome. Biophysical Journal, 2013, 104, 16a.   | 0.5 | 0         |
| 67 | Structural Polymorphism of F-Actin is Coupled with its Mechanical Properties. Biophysical Journal, 2013, 104, 644a-645a.   | 0.5 | 0         |
| 68 | Rate Estimates from Sampling Sparse Transitions: TRNA Motion Limits Transitions between Ribosomal<br>Translocation Intermediates. Biophysical Journal, 2013, 104, 663a.                        | 0.5 | 0         |
| 69 | Rapid and Stable Transfer RNA Translocation through the Ribosome Ensured by Specific Contact<br>Mechanisms. Biophysical Journal, 2014, 106, 493a.  | 0.5 | 0         |
| 70 | Ribosomal Kinetics and Concerted Motions from Nanoseconds to Seconds. Biophysical Journal, 2014,<br>106, 250a.   | 0.5 | 0         |
| 71 | Cryo-Electron Microscopy of Potassium Channel Membrane Proteins. Microscopy and Microanalysis, 2014, 20, 1206-1207.  | 0.4 | 0         |